Proceedings 10th NUMGE 2023
10th European Conference on Numerical Methods in Geotechnical Engineering
Zdravkovic L, Kontoe S, Taborda DMG, Tsiampousi A (eds)

https://doi.org/10.53243/NUMGE2023-417

Stability assessment of dual circular tunnels with different diameters along Hoek-Brown rock masses

S. Sahu[1], G. Tiwari[1], J.P. Sahoo[1]

[1]*Department of Civil Engineering, Indian Institute of Technology Kanpur, India*

ABSTRACT: This paper presents the stability of dual circular shaped tunnels with different diameters in rock masses under surcharge loading on the ground surface using Finite Element Limit Analysis (FELA). The length of the tunnel laid in the rock media is assumed to be enormously large as compared to its lateral dimensions such that the plane strain condition prevails for the current study. The rock mass is modeled as perfectly plastic material obeying the associated flow rule and governed by the non-linear Hoek-Brown failure criterion. In addition, the rock media is assumed to be homogenous and isotropic. For the current studied problem, the maximum value of the surcharge load is estimated for different values of overburden ratio using lower bound FELA. The obtained results are presented in the form of stability charts taking into consideration of different dimensionless parameters. Moreover, the results have been duly validated from the literature for circular tunnels with equal diameters in the rock mass.

Keywords: Circular tunnels; Hoek-Brown failure criterion; Plane strain; Rock mass; Surcharge

1 INTRODUCTION

Construction of underground tunnels has taken a major boost in the current scenario due to rapid urbanization, surface space constraints and congestion. Tunnel stability is one of the major issues which depends on many parameters such as the type and the condition of the geomaterials, presence of joints, faults, shear planes in case of rocks, speed of tunnel boring machine (TBM) and even the adjoining nearby underground structures. Hence, it is necessary to assess the stability of tunnels and underground structures to negate the effect of any potential catastrophes that may happen during the onset of the tunneling process or a long way down the line, i.e., long-term stability. Some famous works related to the stability of tunnels in rock masses have been accomplished. Yang and Huang (2011) used the upper bound limit analysis (UBLA) technique to ascertain the stability of a single circular tunnel in rock mass obeying the Hoek-Brown failure criterion supported from inside by using an isotropic compressive pressure throughout the periphery of the tunnel. Suchowerska et al. (2012) studied the stability analysis of a rectangular tunnel in a rock mass obeying the generalized Hoek-Brown criterion using both the elastoplastic finite element method and the finite element limit analysis method. Ukritchon and Keawsawasvong (2019a, 2019b), by incorporating semidefinite programming (SDP) in conjunction with FELA**,** studied the stability of square tunnels and plane strain headings in rock masses obeying Hoek-Brown failure criterion. Zhang et al. (2019) and Xiao et al. (2019) investigated the stability of dual circular and square-shaped tunnels subjected to surcharge loading at the ground surface using adaptive finite element limit analysis (AFELA) in Hoek-Brown rock masses respectively. Rahaman and Kumar (2020) analyzed the stability of twin horseshoe-shaped tunnels in Hoek-Brown rock masses subjected to surcharge loading using FELA in conjunction with power cone programming (PCP). Most recently, Xiao et al. (2021) used the AFELA to perform a comprehensive study on the stability of unlined rectangular tunnels in rock masses.

It seems that the stability of dual circular shaped tunnels with unequal diameters in rock masses subjected to surcharge loading on the ground surface has not been investigated yet, which should be considered carefully since at times depending upon the geographical locations dual tunnels with unequal geometry may be a viable option. This paper investigates the stability of circular-shaped tunnels with unequal diameters in rock mass that obeys the Hoek-Brown failure criterion subjected to surcharge loading on the ground surface using lower bound finite element limit analysis (LB-FELA).

2 PROBLEM STATEMENT AND METHODOLOGY

Figure 1 depicts the pictorial model for the dual circular tunnels with unequal diameter in a rock mass considering plane strain conditions prevail. Two circular tunnels with a diametrical ratio (D/D') are located below the horizontal ground surface at a depth of C. The central spacing between the centre of the two tunnels is defined as X. A uniformly distributed surcharge (σ_s) is applied on the ground surface which

needs to be optimized. The rock mass is modeled as a perfectly plastic material that obeys the associated flow rule and is governed by the non-linear Hoek-Brown failure criterion. In addition, the rock media is assumed to be homogenous and isotropic having unit weight (γ), uniaxial compressive strength (σ_{ci}), the Geological Strength Index (*GSI*) and the material constant (m_i). The most updated version of the generalized Hoek-Brown failure criterion proposed by Hoek and Brown (2019) is considered in this current study, which can be described as

$$\sigma_1' = \sigma_3' + \sigma_{ci}\left(m_b \frac{\sigma_3'}{\sigma_{ci}} + s\right)^{\alpha} \quad (1)$$

where σ_1' and σ_3' are the major and minor principal stresses respectively and m_b, s, α are the parameters that depend solely on the *GSI* of the rock mass which are represented as follows

$$m_b = m_i * exp\left(\frac{GSI-100}{28-14D^*}\right) \quad (2)$$

$$s = exp\left(\frac{GSI-100}{9-3D^*}\right) \quad (3)$$

$$\alpha = \frac{1}{2} + \frac{1}{6}\left(exp\left(\frac{-GSI}{15}\right) - exp\left(\frac{-20}{3}\right)\right) \quad (4)$$

where, *D** is the disturbance factor which varies from 0 for in-situ completely undisturbed rock masses to 1 for completely disturbed and broken rock masses.

In the current study, a non-dimensional stability number σ_s/σ_{ci} is represented as a function of *C/D, D/D', X/D, GSI,* m_i, $\sigma_{ci}/\gamma D$, *D**

$$\frac{\sigma_s}{\sigma_{ci}} = f\left(\frac{C}{D}, \frac{D}{D'}, \frac{X}{D}, GSI, m_i, \frac{\sigma_{ci}}{\gamma D}, D^*\right) \quad (5)$$

The m_i values varied from 5 to 35 in the interval of 10s. The magnitude of *D/D'* ranges from 1.5 to 4 and *X/D* ranges till the tunnels almost behave independently as single tunnels without the influence of adjacent tunnels. The magnitude of *C/D* varies from 1 to 5, and the value of $\sigma_{ci}/\gamma D$ varies from 50 to 10,000. For simplicity, the disturbance factor (*D**) has been taken as 0 for the current study.

The current study is performed taking into account the plane strain LB-FELA formulation of Sloan (1988). The complete domain is discretized into smaller triangular elements. At each node, three nodal stress (σ_x, σ_y, τ_{xy}) are assigned which are unknown quantities. The surcharge is optimized ensuring a statically admissible stress field by imposing LB constraints namely equilibrium conditions, stress boundary conditions, stress discontinuity conditions along a common edge of two adjacent triangular elements and yield condition throughout the entire domain. For the current study, the lower bound results are obtained taking into account the shear dissipation for mesh adaptivity using OptumG2.

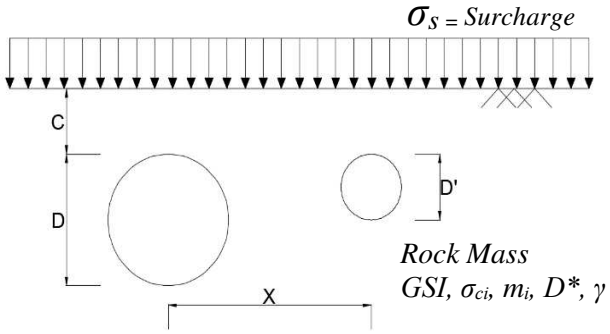

Figure 1. Problem definition of two closely spaced circular tunnels with different diameters in the rock mass

3 VERIFICATION AND COMPARISON OF THE PRESENT ANALYSIS

For validation, considering the case for dual circular tunnels with equal diameters in rock masses subjected to surcharge loading, the current results obtained from lower bound finite element limit analysis taking into account the shear dissipation for mesh adaptivity using OptumG2 are compared with those of Zhang et al. (2019) using adaptive finite element limit analysis approach based on Generalized Hoek-Brown failure criterion. The comparison of results has been presented in Table 1 for the case *C/D* = 1, $\sigma_{ci}/\gamma D$ = 50, D/D'=1, *D** = 0 for *GSI* of 50 and m_i = 5, 15, 25, 35. The results obtained are in good agreement with those of Zhang et al. (2019).

4 RESULTS AND DISCUSSIONS

The lower bounds results for stability number have been determined for the current study. In the subsequent section, detailed discussions have been carried out with respect
to the variation of the stability number with different rock masses and geometrical properties.

Table 1. Stability number (σ_s/σ_{ci}) for circular tunnels with equal diameter having C/D=1, $\sigma_{ci}/\gamma D$ =50, D/D' =1

GSI	X/D	m_i							
		Present Study				Zhang et al. (2019)			
50		5	15	25	35	5	15	25	35
	1.50	0.141	0.283	0.515	0.656	0.139	0.281	0.514	0.640
	1.75	0.148	0.356	0.601	0.873	0.147	0.354	0.601	0.843
	2.00	0.167	0.453	0.792	1.092	0.165	0.452	0.788	1.061
	2.25	0.192	0.562	0.901	1.242	0.191	0.561	0.899	1.234
	2.50	0.262	0.644	1.070	1.510	0.262	0.644	1.052	1.496
	2.75	0.281	0.753	1.201	1.767	0.280	0.752	1.198	1.765
	3.00	0.302	0.825	1.386	1.948	0.302	0.823	1.371	1.945
	3.25	0.304	0.837	1.436	1.976	0.304	0.835	1.410	1.956
	3.50	0.306	0.856	1.451	1.983	0.305	0.854	1.450	1.981
	3.75	0.306	0.856	1.451	1.984	0.305	0.854	1.450	1.981
	4.00	0.306	0.856	1.451	1.984	0.305	0.854	1.450	1.981

**D = Diameter of the larger tunnel*
D' = Diameter of the smaller tunnel

4.1 Analysis of stability number (σ_s/σ_{ci})

4.1.1 Variation of stability number with rock mass properties

In this section, the influence of different rock mass properties namely *GSI*, m_i, $\sigma_{ci}/\gamma D$ on the stability number (σ_s/σ_{ci}) has been presented. Figure 2(a-b) shows the variation of stability number with $\sigma_{ci}/(\gamma D)$ for *D/D'* = 1.5, *X/D* = 2, *C/D* = 1 and 5 for two extreme values of m_i i.e. 5 and 35. For this case, the five values of $\sigma_{ci}/(\gamma D)$ have been considered 50, 100, 500, 1000 and 10000. The results have been presented for *GSI* values of 50 and 70. The figures reveal that the variation of $\sigma_{ci}/\gamma D$ has a very negligible impact on the stability number. The σ_{ci} more or less acts as a multiplier to the stability number and the variation is linear. Similar trends have also been reported by Zhang et. al.(2019) for circular tunnels with equal diameters and later on by Rahaman and Kumar (2020) for twin horseshoe-shaped tunnels in rock masses.

4.1.2 Variation of stability number with different geometrical properties

This section shows the influence of spacing between the centres (*X/D*) and the diametrical ratio (*D/D'*) of the circular-shaped tunnels with unequal diameters on the stability number (σ_s/σ_{ci}). Figures 3(a-b) illustrate the variation of stability number (σ_s/σ_{ci}) with diametrical ratio (*D/D'*) for $\sigma_{ci}/(\gamma D)$ = 100, *X/D* = 2, *C/D* = 1 and 5 for two values of m_i i.e. 5 and 35 and three *GSI* values namely 50, 60, 70.

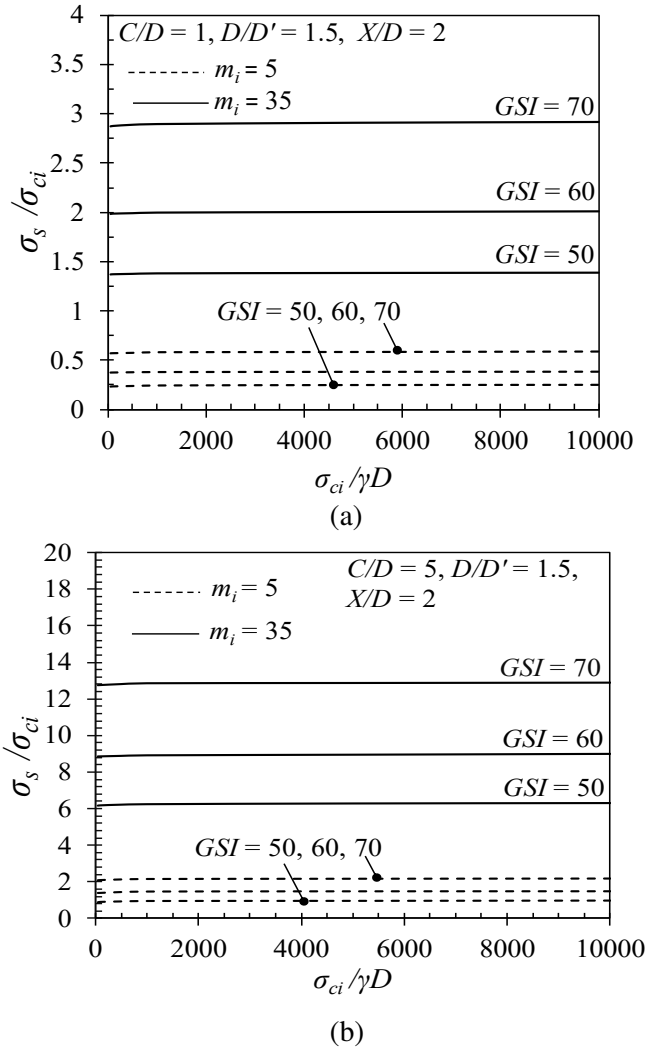

Figure 2. The effect of $\sigma_{ci}/(\gamma D)$ on σ_s/σ_{ci} for (a) C/D = 1 and (b) C/D = 5. Here, m_i = 5, 35, GSI = 50, 60,70, D/D' = 1.5, and X/D = 2.

Five diametrical ratios (*D/D'*) are considered namely 1.5, 2, 2.5, 3 and 4 to illustrate the trend between stability number and diametrical ratio. The trend gives the stability number(σ_s /σ_{ci}) increases for a higher diametrical ratio (*D/D'*) for a given *GSI* and material constant (m_i). For higher material constants, the graph is more evident of higher stability for larger diametrical ratios as compared to low material constant. To conclude, the surcharge carrying capacity increases for unidentical circular tunnels. Moreover, with a higher overburden ratio (*C/D*) the stability number (σ_s /σ_{ci}) increases substantially.

The centre to centre distance between the tunnel plays an important role in estimating the surcharge carrying capacity of the given rock masses. Figures 4 and 5 provide the variation of stability number (σ_s /σ_{ci}) with the centre to centre distance (*X/D*) between circular tunnels with unequal diameters for the *GSI* values of 50 and 70.

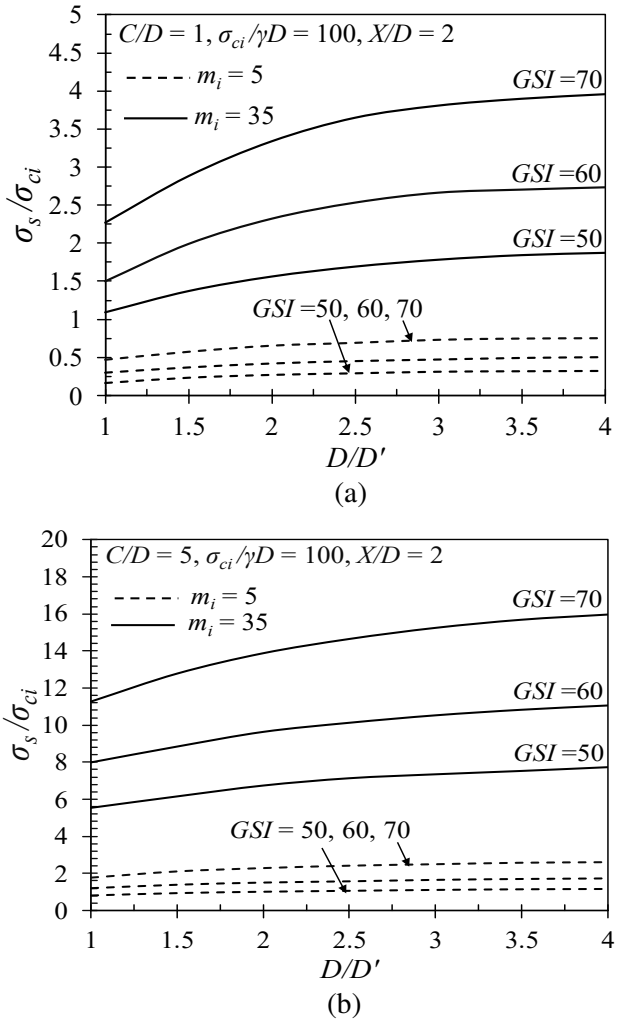

Figure 3. The variation of σ_s/ σ_{ci} with diametrical ratio (D/D') for (a) C/D = 1 and (b) C/D = 5. Here, m_i = 5, 35, GSI = 50, 60,70, σ_{ci} /(γD) = 100, and X/D = 2.

From these figures, it is very clear that with an increase in values of material constant, *GSI* and central spacing between the tunnels, the stability number is increasing and the variation is nonlinear. For an overburden ratio (*C/D*) of 1, after the central spacing exceeds the value 3, the stability number (σ_s /σ_{ci}) becomes constant whereas for greater overburden ratio (*C/D*) the central spacing is large enough to arrive at the zone of constant stability number (σ_s /σ_{ci}). This suggests that when the central spacing becomes greater than or equal to three times the diameter of the larger tunnel, both tunnel behaves independently for *C/D* =1. Similar trends have also been reported by Zhang et al. (2019) for circular tunnels with equal diameters but for circular tunnels with unequal diameters, the stability numbers (σ_s /σ_{ci}) are found to be higher as compared to equal diameter circular tunnels for lower spacings between the tunnels.

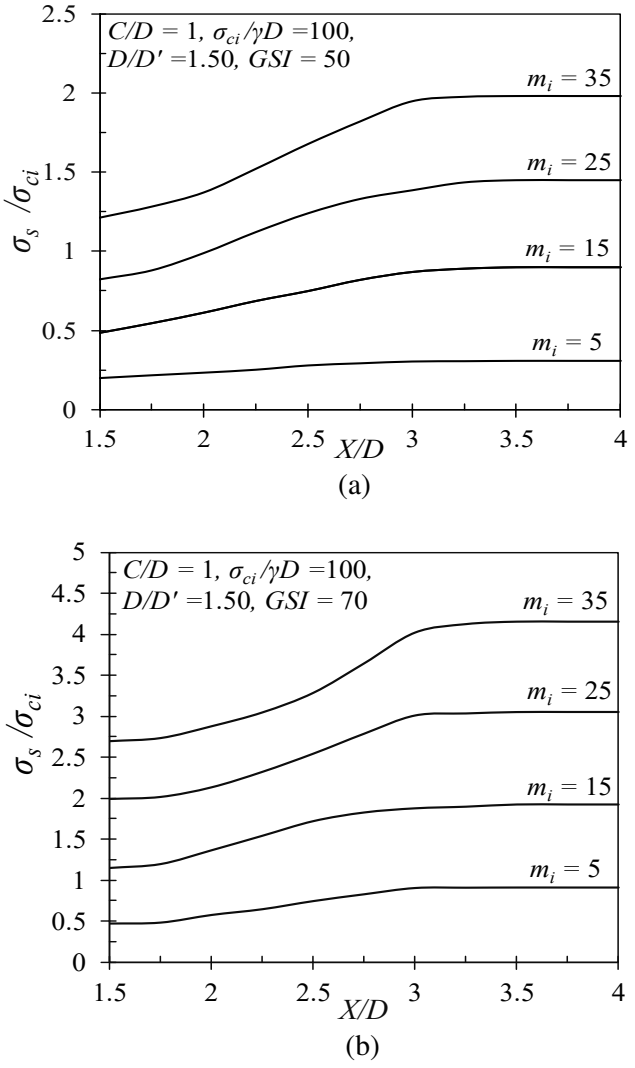

Figure 4. The variation of σ_s / σ_{ci} with the centre to centre spacing (X/D) for (a) GSI = 50 and (b) GSI = 70. Here, m_i = 5, 15, 25, 35, D/D' = 1.50, σ_{ci} / γD = 100, and C/D = 1.

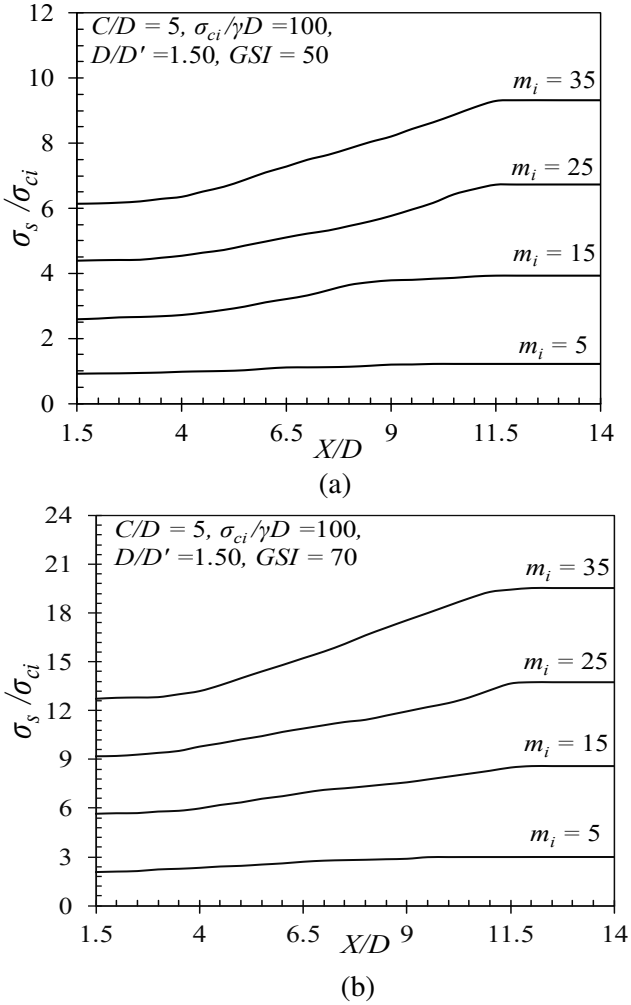

Figure 5. The variation of σ_s / σ_{ci} with the centre to centre spacing (X/D) for (a) GSI = 50 and (b) GSI = 70. Here, m_i = 5, 15, 25, 35, D/D′ = 1.50, $\sigma_{ci} / \gamma D$ = 100, and C/D = 5

4.1.3 Failure patterns

Figure 6 represents the failure pattern for the circular tunnel with equal diameters for overburden ratio (*C/D*) of 1. It clearly represents that for lesser separation between the tunnels, the failure zone tends to overlap due to which the stability number is less for closely spaced tunnels as compared to distantly spaced tunnels where there is no zone of overlap and both tunnels behave as two independent tunnels in rock masses. Figure 7(a-b) represents the failure patterns for circular-shaped tunnels with unequal diameters in rock masses. It is clear from the failure pattern that the larger tunnel is the major governing parameter because the failure zone profoundly extends up to the ground surface for the larger one compared to the smaller one. Since for smaller tunnels, the failure zone is restricted which might be one of the possible reasons behind the enhancement of the stability number for unlike-shaped tunnels. From Figure 7(b) it is clear that as the centre to centre distance increases there exists no zone of overlap.

Note that the distributions represent the inequality yield constraint as follows

$$(\sigma_1' - \sigma_3') - \sigma_{ci}\left(m_b \frac{\sigma_3'}{\sigma_{ci}} + s\right)^{\alpha} \leq 0 \qquad (6)$$

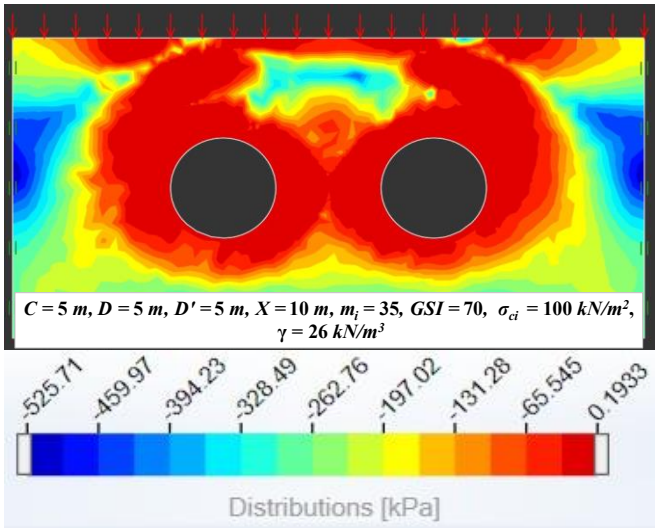

Figure 6. Failure plot for circular tunnels with equal diameters. Here, GSI = 70, m_i=35 σ_{ci} = 100 kN/m², C =5 m, D = 5 m, D′ = 5 m, γ = 26 kN/m³, X = 10 m.

5 CONCLUSIONS

The stability of dual circular shaped tunnels with unequal diameters in rock masses obeying the Hoek-Brown failure criterion subjected to surcharge loading has been studied by using lower bound finite element limit analysis. The dimensionless stability number (σ_s / σ_{ci}) are presented in form of design charts for engineers to use. Based on the results of the current study, the major conclusions that can be drawn are as follows:

1. The variation of the stability number (σ_s / σ_{ci}) increases continuously with incremental values of *GSI* and m_i, while the stability number (σ_s / σ_{ci}) ceases to vary with the factor $\sigma_{ci} / \gamma B$.
2. A critical point for the spacing to diameter (*X/D)* can be defined for circular tunnels with unequal diameters, which depends on the overburden ratio (*C/D*). The higher the overburden ratio (C/D), the greater will be the critical point. In the current study, the critical point is noted to be around 3 and 11 for C/D ratio of 1 and 5 respectively.
3. The variation of the stability number (σ_s / σ_{ci}) for higher diametrical ratio (*D/D′*) becomes constant after a certain critical point but there is an increment in surcharge carrying capacity for

circular tunnels with unequal diameters as compared to the circular tunnels with equal diameters having $D/D' = 1$.

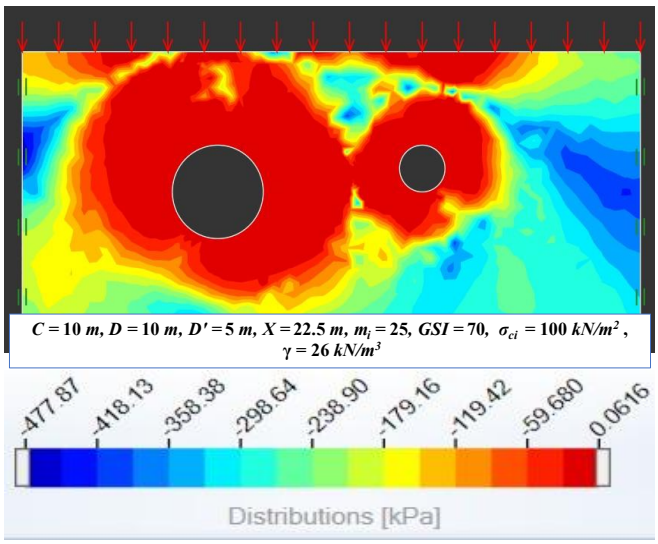

(a)

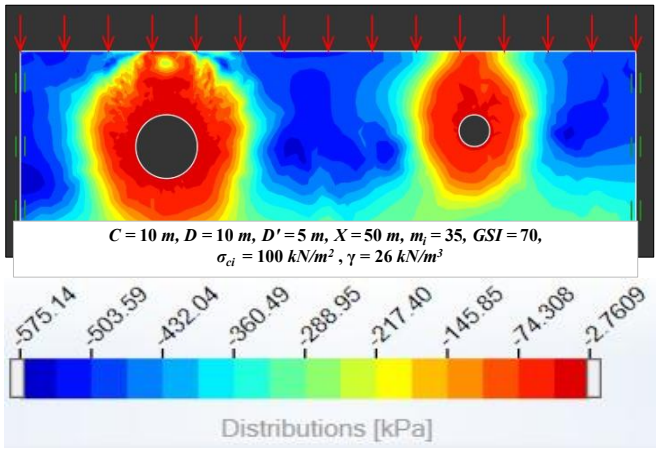

(b)

Figure 7. Failure plot for circular tunnels with unequal diameters with (a) X/D = 2.25 (m_i=25) (b) X/D = 5 (m_i=35). Here, GSI = 70, σ_{ci} = 100 kN/m², C =10 m, D = 10 m, D' = 5 m, γ = 26 kN/m³.

6 REFERENCES

Hoek, E., & Brown, E. T. 1980. Empirical Strength Criterion for Rock Masses. *Journal of the Geotechnical Engineering Division*, ***106*****(9)**, 1013–1035.

Hoek, E., & Brown, E. T. 2019. The Hoek–Brown failure criterion and GSI – 2018 edition. *Journal of Rock Mechanics and Geotechnical Engineering*, ***11*****(3)**, 445–463.

Keawsawasvong, S., Ukritchon, B. 2020. Design equation for stability of shallow unlined circular tunnels in Hoek-Brown rock masses. *Bulletin of Engineering Geology and the Environment*, ***79*****(8)**, 4167–4190.

Rahaman, O., Kumar, J. 2020. Stability analysis of twin horse-shoe shaped tunnels in rock mass. *Tunnelling and Underground Space Technology*, ***98***.

Sloan, S. W. 1988. Lower bound limit analysis using finite elements and linear programming. *International Journal for Numerical and Analytical Methods in Geomechanics*, ***12*****(1)**, 61–77.

Suchowerska, A. M., Merifield, R. S., Carter, J. P., Clausen, J. 2012. Prediction of underground cavity roof collapse using the Hoek–Brown failure criterion. *Computers and Geotechnics*, ***44***, 93–103.

Ukritchon, B., Keawsawasvong, S. 2019a. Stability of unlined square tunnels in Hoek-Brown rock masses based on lower bound analysis. *Computers and Geotechnics*, ***105***, 249–264.

Ukritchon, B., Keawsawasvong, S. 2019b. Lower bound stability analysis of plane strain headings in Hoek-Brown rock masses. *Tunnelling and Underground Space Technology*, ***84***, 99–112.

Xiao, Y., Zhang, R., Zhao, M., Jiang, J. 2021. Stability of Unlined Rectangular Tunnels in Rock Masses Subjected to Surcharge Loading. *International Journal of Geomechanics*, ***21*****(1)**.

Xiao, Y., Zhao, M., Zhang, R., Zhao, H., Wu, G. 2019. Stability of dual square tunnels in rock masses subjected to surcharge loading. *Tunnelling and Underground Space Technology*, ***92***, 103037.

Yang, X. L., Huang, F. 2011. Collapse mechanism of shallow tunnel based on nonlinear Hoek–Brown failure criterion. *Tunnelling and Underground Space Technology*, ***26*****(6)**, 686–691.

Zhang, J., Feng, T., Yang, J., Yang, F., Gao, Y. 2018. Upper-bound stability analysis of dual unlined horseshoe-shaped tunnels subjected to gravity. *Computers and Geotechnics*, ***97***, 103–110.

Zhang, R., Xiao, Y., Zhao, M., Zhao, H. 2019. Stability of dual circular tunnels in a rock mass subjected to surcharge loading. *Computers and Geotechnics*, ***108***, 257–268.